J Mater Sci (2010) 45:897–905
DOI 10.1007/s10853-009-4017-3

Preparation and structural studies in the $(70 - x)TeO_2$–$20WO_3$–$10Li_2O$–xLn_2O_3 glasses

I. Z. Hager · R. El-Mallawany

Received: 21 April 2009 / Accepted: 3 November 2009 / Published online: 24 November 2009

Abstract Quaternary tellurite glass systems $(70 - x)TeO_2$–$20WO_3$–$10Li_2O$–xLn_2O_3 where $x = 0$, 1, 3 and 5 mol% and Ln are La, Pr, Nd, Sm, Er and Yb, respectively, have been prepared by the melt quenching technique. Densities of the obtained glasses were measured and the molar volume was calculated. IR absorption spectra of the present glass systems were determined at room temperature over the range of wavenumbers from 400–1,600 cm^{-1}. Raman spectra of the present glass samples were measured in the range of 30–1,030 cm^{-1}. Density, molar volume, IR and Raman spectra of the glasses were discussed by calculating average cross-link density, packing density, theoretically calculated Poisson's ratio and number of bonds per unit volume of the studied glasses. Also, the quantitative interpretations were based on concentration of ions per unit volume of *Te*, *Ln* and *O*, short distance in nanometre between ions for (Te–O) of TeO_4 and TeO_3 groups, (W–O) of WO_4, WO_6 groups and calculated wavenumber, $\bar{\upsilon}$, for TeO_4 and TeO_3, respectively. The average stretching force constant that present in these quaternary glasses has been calculated in order to interpret the data obtained.

Introduction

Structural studies in glasses are of great important owing to the interrelation between the atomic arrangement and properties. While this interest is primarily on the technological side, structural on glasses offer a unique possibility to evaluate theories and structural models developed over the last decades [1]. To comprehend structural details, a common strategy is to change the glass structure either by adding network modifiers or by interrogating the material with some external stimuli such as heat or pressure. Tellurium oxide is an interesting case where the basic building block of structure experiences considerable changes either by modifiers or by increasing temperature, though being of three-dimensional geometry. Tellurite-oxide based glasses have been considered as promising materials for use in non-linear optical devices or host materials for upconversion fluorescence of rare earth ions [2–10]. They are characterized by high refractive index values (larger than 2.0 in most cases) [11], wide infrared transmittance [12], high thermal expansion and good chemical durability. So, it is of interesting to investigate the structure of the tellurite glass especially when the glass doped with different rare earth ions. Crystalline TeO_2 has a unique structural unit that is, an asymmetrical TeO_4 trigonal bipyramid (tbp), in which there are two different kinds of sites, two axial and three equatorial positions. One of the latter is occupied by a lone pair of electrons. The structural of TeO_2 based glasses is of interest, because there are two types of basis structural unit, i.e. TeO_4 tbp with a lone pair electron in an equatorial position and TeO_3 trigonal pyramid (tp). The tellurite glass system is an important amorphous system considered to have important commercial applications in optical communication due to its high refractive index, good infrared transmittance and high optical non-linearity. Tellurite glass is a good host material for laser applications. Tellurite glasses doped with rare earth ions are also candidates for excitations, absorption, photoluminescence at different colors as mentioned previously [8, 9].

In the present work, the structure of the prepared glass system $(70 - x)TeO_2$–$20WO_3$–$10Li_2O$–xLn_2O_3 where

I. Z. Hager (✉) · R. El-Mallawany
Physics Department, Faculty of Science, Menoufia University, Shebin El-Koom, Egypt
e-mail: izhager@yahoo.com

$x = 0$, 1, 3 and 5 mol.% Ln: La, Nd, Sm, Er, Yb and Pr_6O_{11} were investigated by using infrared and Raman spectroscopy in addition of density and molar volume. Also the structure of the glasses is interpreted by calculated parameters like average cross-link density, Poisson's ratio, number of bonds per unit volume, bond length and stretching force constant. The effect of the concentration of the added rare earth ions on the structure, calculated and measured parameters is discussed.

Experimental technique

Glass preparation

The raw materials which used (TeO_2 from Alfa, $LiCO_3$ and WO_3 from Strem and rare earth oxides are from Prolabo) were of Analar Grade. The batches were melted at a maximum temperature of ~950 °C in a deep platinum crucible for 30–45 min in air. Then they could be poured into a heated brass mould to obtain cubic samples with dimensions about $1 \times 1 \times (0.6–1.0)$ cm^3. The samples were annealed at ~250–300 °C for 1 h. The samples were also polished and prepared for the measurements.

The densities of the prepared samples were measured by the Archimedean method using CCl_4 as an immersion liquid. The molar volume was calculated by the equation $V_m = (M/\rho)$, where ρ is the density and M the molecular weight of the glass sample, which is calculated as follows: $M = \sum_i (x_i)(w_i)$, where x_i and w_i are the mole fraction and molecular weight of the component i, respectively. The error of the density measurements was not more than ±0.001.

IR measurements

For infrared investigations, glass sample was ground in a clean mortar to fine powder. Fixed weight from glass powder and KBr (from Prolabo) were mixed and ground. Then transparent pellets were formed by pressing the mixture at 10 tons for a few minutes under vacuum. IR absorption spectra of the present glass systems were determined by using a Bomem Michelson 100 spectrophotometer. All measurements were carried out at room temperature over the range of wavenumbers from 400 to 1,600 cm^{-1}.

Raman spectra measurements

Raman spectra of the present glass samples with two polished faces and approximately 6–10 mm in thickness were measured in the range of 30–1,030 cm^{-1} by using Olympus BHT microscope with ×50 LF and ×100 objectives and the spectra are analyzed with a Dilor Z24 Raman spectrometer (single channel, triple monochromator) equipped with a photo-multiplier; an argon ion laser Coherent Innova 90-3. The Raman spectra were measured at university of Le Mans, France.

Results and discussion

Density and structure parameters

The compositions of the studied glasses are given in Table 1. The values of the glass density and molar volume of the present tellurite glass doped with various rare earth oxides are given in Table 2. The density values are comparable to those previously measured (5.88–6.18 g/cm^3) [13]. Figure 1a shows the variation of the glass density with the concentration of the rare earth oxides. It is seen that the density increase with increasing the rare earth oxides content. The density of Yb, Er and Pr doped glasses is higher than those of Sm, Nd and La doped glasses. The increase in the density is attributed to that the molecular weight of the added rare earth oxides (more than 300) is higher than that of TeO_2 (159.59). The molar volume increased with increasing the rare earth oxide contents as shown in Fig. 1b. The observed increase in the molar volume may be attributed to an increase in the bond length or the inter-atomic spacing between the atoms as given in Table 4. The density of the glasses can be estimated from the density of their constituents according to this equation:

$$\rho = \sum_i x_i \rho_i, \tag{1}$$

where x_i is the mole fraction of the component i and ρ_i its density. The calculated and the measured values are in good agreements as collected in Table 2.

It is of interesting to calculate the average crosslink density of the present glasses, which is calculated according to this equation:

$$\bar{n_c} = \frac{1}{\eta}[(n_c)_1(N_c)_1 + (n_c)_2(N_c)_2 + \cdots] \tag{2}$$

where $n_c = n_f - 2$, n_f is the coordination number of the glass component, which equals 4 for TeO_2 and Li_2O, 6 for WO_3, Er_2O_3 and Yb_2O_3, 7 for Nd_2O_3, Sm_2O_3, La_2O_3 and Pr_6O_{11}, respectively.

$$\eta = \sum_i (N_c)_i = \sum_i x_i n_i$$

and n_i is the number of cations of the component i. The calculated values of $\bar{n}_c$ are given in Table 2.

The increase in the average crosslink density from 2.364 to 2.609 means that the addition of rare earth

Table 1 The composition of the prepared $(70 - x)TeO_2$–$20WO_3$–$10Li_2O$–xLn_2O_3 glass systems

Sample name	TeO_2	WO_3	Li_2O	La_2O_3	Pr_6O_{11}	Nd_2O_3	Sm_2O_3	Er_2O_3	Yb_2O_3
TWL	70	20	10						
TWLLa1	69	20	10	1					
TWLLa2	67	20	10	3					
TWLLa3	65	20	10	5					
TWLPr1	69	20	10		1				
TWLPr2	67	20	10		3				
TWLPr3	65	20	10		5				
TWLNd1	69	20	10			1			
TWLNd2	67	20	10			3			
TWLNd3	65	20	10			5			
TWLSm1	69	20	10				1		
TWLSm2	67	20	10				3		
TWLSm3	65	20	10				5		
TWLEr1	69	20	10					1	
TWLEr2	67	20	10					3	
TWLEr3	65	20	10					5	
TWLYb1	69	20	10						1
TWLYb2	67	20	10						3
TWLYb3	65	20	10						5

Table 2 The density (measured and calculated), molar volume, average cross-link density, packing density, theoretically calculated Poisson's ratio and number of bonds per unit volume of the studied glasses

Sample no.	ρ (gm/cm^3) (measured)	ρ (gm/cm^3) (calculated)	V_m (cm^3)	$\overline{n_c}$	$V_t \times 10^{-6}$ m^3	μ_{cal} (calculated)	$n_b \times 10^{21}$ cm^{-3}
TWL	5.760	5.771	27.96	2.364	1.209	0.385	103.382
TWLLa1	5.783	5.777	28.14	2.414	1.197	0.384	104.656
TWLLa2	5.823	5.789	28.52	2.513	1.173	0.382	106.756
TWLLa3	5.840	5.801	29.00	2.609	1.144	0.379	108.504
TWLPr1	5.823	–	29.14	2.414	1.179	0.382	104.917
TWLPr2	5.900	–	31.68	2.513	1.119	0.376	106.719
TWLPr3	5.944	–	34.35	2.609	1.064	0.369	107.721
TWLNd1	5.788	5.785	28.14	2.414	1.197	0.384	104.861
TWLNd2	5.829	5.812	28.54	2.513	1.170	0.381	107.610
TWLNd3	5.853	5.838	29.03	2.609	1.141	0.378	109.944
TWLSm1	5.792	5.788	28.14	2.414	1.197	0.384	104.861
TWLSm2	5.832	5.822	28.59	2.513	1.168	0.381	107.423
TWLSm3	5.888	5.856	28.96	2.609	1.143	0.378	110.209
TWLEr1	5.816	5.799	28.08	2.396	1.199	0.384	104.861
TWLEr2	5.900	5.853	28.43	2.460	1.173	0.382	107.687
TWLEr3	5.968	5.908	28.86	2.522	1.144	0.379	110.057
TWLYb1	5.834	5.804	28.01	2.396	1.203	0.385	107.049
TWLYb2	5.911	5.870	28.44	2.460	1.175	0.382	112.913
TWLYb3	5.944	5.936	29.07	2.522	1.141	0.378	117.459

oxides to present TWL (TeO_2–WO_3–Li_2O) glass modify Te–O–Te by decreasing the tellurium atom coordination number from 4 to 3. This leads to creation of extra bridging oxygen atoms and increase the connectivity of the network [14]. This leads to increase the density as shown in Fig. 1a.

The Poisson's ratio can be also calculated theoretically from the expression given by [15]:

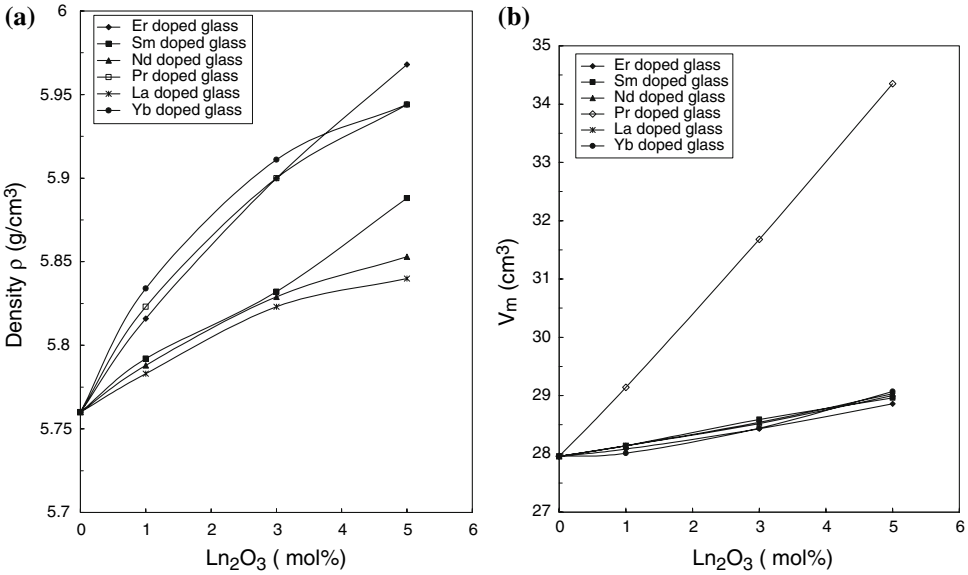

Fig. 1 **a** Variation of the density with composition of TeO_2–WO_3–Li_2O glass doped with rare earth oxides. **b** Variation of molar volume with composition of TeO_2–WO_3–Li_2O glass doped with rare earth oxides

$$\mu_{\text{cal}} = 0.5 - \frac{1}{7.2\,V_t} \tag{3}$$

where

$$V_t = \frac{\rho}{M}\sum_i x_i V_i \tag{4}$$

and

$$V_i = \frac{4\pi N}{3}(nR_A^3 + mR_O^3), \tag{5}$$

where μ_{cal} is the theoretically calculated Poisson's ratio, V_t the packing density of the glass, ρ the glass density, M the glass molecular weight, x_i the mole fraction of the component i, V_i the packing factor of the oxide A_nO_m, N the Avogadro's number, R_A and R_O are the ionic radius of cation A and anion O, respectively.

The calculated packing factor for TeO_2, WO_3 and Li_2O is equal to 41.05×10^{-6}, 21.42×10^{-6}, 8.01×10^{-6} m^3 while equal to 25.22×10^{-6}, 26.43×10^{-6}, 27.11×10^{-6}, 28.03×10^{-6}, 28.42×10^{-6} and 95.69×10^{-6} m^3 for Er_2O_3, Sm_2O_3, Nd_2O_3, Yb_2O_3, La_2O_3 and Pr_6O_{11}, respectively. So, by increasing the rare earth oxides with packing factor less than that of TeO_2, the packing density V_t of the glasses decreases and the calculated Poisson's ratio also decreased.

It is obtained that by increase the rare earth oxides instead of TeO_2 the Poisson's ratio, μ_{cal}, decrease from 0.385 of the blank sample (which undoped with rare earth (TWL)) to around 0.369 for the samples doped with rare earth oxides, Table 2. It is known that Poisson's ratio is affected by the changes in the cross-link density of the glass network [16]. Which means that, the decrease in μ_{cal} is attributed to the increase in the cross-link density, which was observed in the present glasses by increasing of the rare earth oxides instead of TeO_2, see Table 2. Also, a high cross-link density has Poisson's ratio in the order of 0.1 to 0.2, while a low cross-link density has Poisson's ratio between 0.3 and 0.5 [14, 17, 18]. Also, the decrease of the calculated Poisson's ratio is attributed as mentioned before to the increase in the connectivity of the network linkages and the strong of the network structure of the glasses by adding the rare earth oxides. This can be interpreted by the number of bonds per unit volume, n_b, of the glasses which calculated as follows:

$$n_b = \sum n_s \frac{N\rho}{M}, \tag{6}$$

where n_s is the number of bonds per unit glass formula, n_s = (coordination number of each cation) × (number of cations in the glass formula unit), N the Avogadro's number, M the glass molecular weight and ρ its density.

The calculated values of n_b are given in Table 2. As obtained from the above relation (6) and Table 2, the number of bonds per unit volume increases, e.g. for the present telluride glasses doped with La_2O_3 by 1 and 5 mol.% the number of bonds per unit volume increased from n_b 104.656–108.504 × 10^{21} cm^{-3}. Therefore, the glasses become more connective and rigid by doping the rare earth oxides into the studied glasses.

IR spectra

IR absorption spectra of the present glasses, undoped and doped with rare earth oxides such as Er_2O_3, La_2O_3, Pr_6O_{11}, Sm_2O_3, Yb_2O_3 and Nd_2O_3 are shown in Fig. 2a–c, respectively. Their assigned band positions are reported in Table 3. From these figures, it is shown that there are different absorption bands which, respectively, 500, 610,

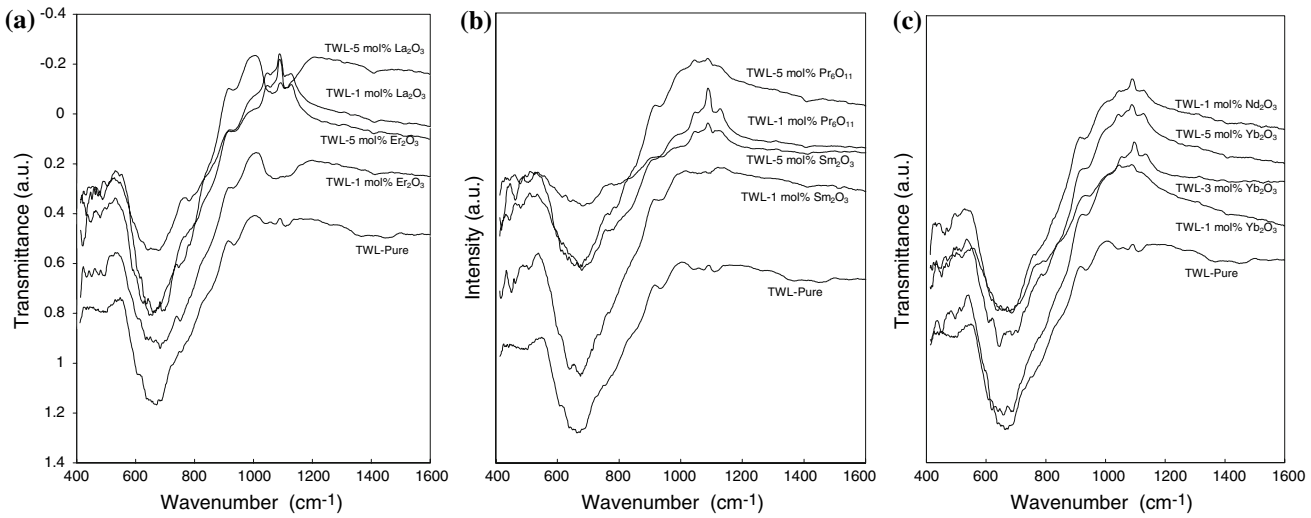

Fig. 2 **a** Infrared absorption spectra of TeO_2–WO_3–Li_2O glasses doped with Er_2O_3 and La_2O_3. **b** Infrared absorption spectra of TeO_2–WO_3–Li_2O glasses doped with Pr_6O_{11} and Sm_2O_3. **c** Infrared absorption spectra of TeO_2–WO_3–Li_2O glasses doped with Yb_2O_3 and Nd_2O_3

Table 3 Infrared absorption band position experimental and calculated of TeO_2–WO_3–Li_2O glasses doped with rare earth oxides

Sample no.	Te–O–W or Ln–O	TeO_3 (meas.) (cm^{-1})	$\bar{\upsilon}_{(calc.)}$ TeO_3 (cm^{-1})	TeO_4 (meas.) (cm^{-1})	$\bar{\upsilon}_{(calc.)}$ TeO_4 (cm^{-1})	TeO_3 (meas.)	WO_4 or WO_6	TeO_4		
TWL		500	564	660	699	745	930	1055	1108	1400
TWLLa1	450	480	558	650	693	780	930	1045	1092	1400
TWLLa2	440		546	655	678	777	930	1045	1100	1400
TWLLa3	430	470	533	660	662	780	930	1045	1107	1400
TWLPr1	460	470	548	680	680	770	925	1045	1092	
TWLPr2	455		510	675	644	780	925	1045	1092	1400
TWLPr3	440	480	490	680	608	770	925	1045	1092	1400
TWLNd1	460	520	558	680	693	770	930	1045	1092	1392
TWLNd2	460	510	546	670	678	760	930	1045	1092	1392
TWLNd3	460	510	558	670	660	760	930	1045	1100	1392
TWLSm1	450	510	548	670	693	770	930	1085		1400
TWLSm2	450		548	665	677	780	930	1055		1400
TWLSm3	460	500	534	670	663	790	930	1045	1100	1400
TWLEr1	430	490	559	660	693	745	925	1060		1400
TWLEr2	435		547	675	679	745	925	1055	1100	1400
TWLEr3	420	490	535	680	664	750	925	1060	1092	1400
TWLYb1	450	490	549	660	682	780	925	1052	1100	1400
TWLYb2	440	510	547	670	679	780	925	1045	1092	1392
TWLYb3	450	520	533	660	661	790	925	1040	1092	1392

660, 780, 930, 1,055, 1,108 and 1,400 cm^{-1} for the sample, which undoped with rare earth oxides. By adding Ln_2O_3 (rare earth oxides) to this sample instead of TeO_2, there are absorption band appeared at 440–470, 480–520, 650–680, 745–790, 930, 1,040–1,085, 1,092–1,107 and 1,492–1,400 cm^{-1}, respectively as shown in Fig. 2a–c. The two bands that at 1,055 and 1,108 cm^{-1} of the undoped sample are combined to be one band at 1,085–1,045 cm^{-1} by adding Sm_2O_3. From these Fig. 2a–c, its observed that, by adding the rare earth oxides to the present glasses instead of TeO_2 the band which at 600 cm^{-1} of the undoped samples with rare earths was combined with the band which at 660 cm^{-1} and shifted to become around 650–680 cm^{-1} as tabulated in Table 3.

According to the IR absorption spectra of the studied glasses, the absorption band which around 430–450,

440–460, 460, 450–460, 420–435 and 440–450 cm^{-1} are assigned to be due to La–O, Pr–O, Nd–O, Sm–O, Er–O and Yb–O stretching vibrations, respectively. This means that a fraction of rare earth ions was incorporated in the network of these glasses and act as a network intermediate. The main broad intense absorption band which at around 660 cm^{-1} for the undoped glass sample and 650–680 cm^{-1} of the glass sample doped with rare earths are assigned to be the bonding mode of Te–O–Te or O–Te–O linkages, the stretching mode [TeO_4] tp with bridging oxygen. It is known that, the addition of different other components to tellurite glasses like WO_3, Li_2O or Ln_2O_3 may cause the vibration of TeO_3 groups around 745–790 cm^{-1} and that symmetric and antisymmetric stretching vibration of TeO_3 groups tp with NBO induces the peak around 745 cm^{-1} [19]. With an increase in rare earth oxides, e.g. La_2O_3 content to TeO_2 based glass, the coordination state of tellurium atom changes from TeO_4 tpb through TeO_{3+1} polyhedra to TeO_3 tp, and NBO atoms increase in number. Glass having low La_2O_3 content have a continuous network structure composed mainly of TeO_4 tpb and TeO_{3+1} polyhedra having one NBO atom, while glasses containing more than 15 mol% La_2O_3 contain small structural fragments composed of TeO_3 tps having two or three NBO atoms [20]. So that the number of NBO in the present glasses is very low, and this is the reason which it called that the glass is rigid and more connective. The peak at 420–460 cm^{-1}, which appears by adding the rare earth oxides to the present glasses, may be due to Ln–O as described before, or Te–O–W bridging bonds, which would increase the network connectivity [21]. The formation of Te–O–W bridging is expected because both W and Te atoms have comparable electronegativity and can therefore substitute for each other in bonding with O atoms [22]. That is a small fraction of W cations, which are incorporated in the glass network. The bands, which at 1,045, 1,092 and 1,100 cm^{-1}, are due to TeO_4 group. While the band at 930 cm^{-1} is due to WO_4 tetrahedral and/or WO_6 octahedral group [23]. It is obtained that most of the absorption band position in general are shifted towards the lower frequency region by doping the rare earth oxides to the present glasses. This is because the rare earth oxides are enter the glass network as intermediate and also it means that tellurite glass are good host material for rare earth ions. This result yields that the present glasses are good host for the rare earth ions for the optical properties studying the optical applications.

In order to calculate the wavenumber band position of the present glasses, we follow the following steps: the short distance between the ions can be calculated from the concentration of the ions A and O of the compound A_nO_m, which given as the following equations [14, 24]:

$$n(A) = \frac{n\,x\,N}{100\,V_m}, \tag{7}$$

$$n(O) = \frac{m\,x\,N}{100\,V_m}, \tag{8}$$

where N, x and V_m are the Avogadro's number, mole fraction of A_nO_m and the glass molar volume respectively. Therefore, the short separation distances, r, between the identical A or O ions are given by:

$$r = \sqrt[3]{\frac{1}{n}} \tag{9}$$

According to Eqs. 7–9, the calculated values of n(Te), n(O), n(W), r(Te–Te), r(O–O) and r(W–W) are given in Table 4. Therefore, r(Te–O) can be calculated for the TeO_4 group by considering the Te ions, which are lying in the centre of four oxygen ions, see Table 4 for the obtained values. Also, r(Te–O) for TeO_3 group can be calculated by considering the Te atom, which is put at the cross-point position of the vertical lines from the vertex of the equal ribs triangle with its vertices are the oxygen atoms, as shown in Table 4 for obtained values. Therefore, the wavenumber position of the vibrated modes can be calculated as follows:

$$\overline{\upsilon} = \frac{1}{2\,\pi\,c}\sqrt{\frac{F}{\mu}} \tag{10}$$

where

$$F = \frac{1.7}{r^3} \tag{11}$$

where c, F, μ and r are the velocity of light, stretching force constant, reduced mass between the cation–anion and r the calculated bond length between them in nanometre. All the calculated parameters are given in Tables 3 and 4, respectively. The calculated wavenumber are reasonably compared with that the measured experimental from IR spectra. Figure 3 shows the dependence of the stretching force constant, F, with the bond length of the Te groups. F decrease with increasing the bond length of main groups. For more structural details, Raman spectroscopy was used as shown in the next section.

Raman spectra

The Raman spectra of some of the present glasses undoped and doped with rare earths reveals also different absorption bands as shown in Fig. 4a, b, respectively. Two main absorption bands at around 700 and 930 cm^{-1} in addition of 480, 360, 220, 132 and 54 cm^{-1}, Table 5. By adding the rare earth oxides to the present glasses, these bands are affected and become at around 695–711, 930, 465–480,

Table 4 The concentration of ions per unit volume of Te, Ln and O, short distance in nm between ions for (Te–Te), (O–O), (Te–O) of TeO_4 and TeO_3 groups, (W–W), (W–O) of WO_4 and WO_6 groups and the stretching force constant in (N/m) for TeO_4 and TeO_3 of the present glasses respectively

Sample no.	n(Te) × 10^{20} cm^{-3}	n(Ln) × 10^{20} cm^{-3}	n(O) × 10^{20} cm^{-3}	r(Te–Te) (nm)	r(O–O) (nm)	r(Te–O) of TeO_4 (nm)	r(Te–O) of TeO_3 (nm)
TWL	150.744	–	452.231	0.405	0.321	0.1610	0.1855
TWLLa1	147.661	4.279	451.541	0.4076	0.3235	0.1617	0.1868
TWLLa2	141.471	12.669	449.749	0.4135	0.3282	0.1641	0.1895
TWLLa3	134.976	20.766	446.459	0.4200	0.3334	0.1667	0.1925
TWLPr1	142.594	12.399	452.579	0.4124	0.3273	0.1637	0.1890
TWLPr2	123.359	34.216	450.509	0.4282	0.3399	0.1699	0.1962
TWLPr3	113.953	52.594	447.048	0.4444	0.3527	0.1764	0.2036
TWLNd1	147.661	4.279	451.541	0.4076	0.3235	0.1617	0.1868
TWLNd2	141.371	12.660	449.434	0.4136	0.3282	0.1641	0.1895
TWLNd3	134.836	20.744	445.997	0.4201	0.3335	0.1668	0.1925
TWLSm1	147.682	4.281	451.607	0.408	0.324	0.162	0.1868
TWLSm2	141.114	12.637	448.617	0.414	0.328	0.164	0.1896
TWLSm3	135.1529	20.793	447.044	0.420	0.333	0.167	0.1924
TWLEr1	147.987	4.289	452.540	0.407	0.323	0.162	0.1866
TWLEr2	141.898	12.707	451.109	0.413	0.328	0.164	0.1893
TWLEr3	135.644	20.868	448.671	0.419	0.333	0.166	0.1921
TWLYb1	148.346	4.299	443.639	0.4069	0.3267	0.1634	0.1886
TWLYb2	141.868	12.705	451.015	0.4131	0.3279	0.1639	0.1893
TWLYb3	134.651	20.715	445.384	0.4203	0.3336	0.1668	0.1926

Sample no.	r(W–W) (nm)	r(O–O) (nm)	r(W–O) of WO_4 (nm)	r(W–O) of WO_6 (nm)	F of TeO_4 (N/m)	F of TeO_3 (N/m)
TWL	0.6232	0.4262	0.2131	0.1507	410	266
TWLLa1	0.6159	0.4315	0.2135	0.1509	402	261
TWLLa2	0.6187	0.4289	0.2144	0.1516	385	250
TWLLa3	0.6222	0.4314	0.2157	0.1525	367	238
TWLPr1	0.6231	0.4321	0.2161	0.1528	387	252
TWLPr2	0.6407	0.4443	0.2222	0.1571	347	225
TWLPr3	0.6582	0.4564	0.2282	0.1614	310	201
TWLNd1	0.6159	0.4315	0.2135	0.1509	402	261
TWLNd2	0.6188	0.4291	0.2146	0.1517	385	250
TWLNd3	0.6223	0.4315	0.2157	0.1525	366	238
TWLSm1	0.6159	0.4270	0.2135	0.1509	402	261
TWLSm2	0.6192	0.4293	0.2147	0.1517	384	249
TWLSm3	0.6218	0.4312	0.2156	0.1524	368	239
TWLEr1	0.6154	0.4267	0.2134	0.1508	403	261
TWLEr2	0.6180	0.4285	0.2143	0.1515	386	251
TWLEr3	0.6211	0.4306	0.2153	0.1522	369	240
TWLYb1	0.6149	0.4264	0.2132	0.1507	390	253
TWLYb2	0.6181	0.4286	0.2143	0.1516	386	251
TWLYb3	0.6226	0.4317	0.2159	0.1526	366	238

339–348, 120–153 and 48–57 cm^{-1} in addition of new band around 735–745 cm^{-1}, respectively, Table 5. It is seen that the band position, which at 930 cm^{-1}, does not changed by adding the rare earth oxides to the present glasses. The peak which at 695–711 cm^{-1} is assigned to be due to the vibration v_1 of TeO_4 group [25], while which at 930 cm^{-1} band is due to v_1 of WO_4 tetrahedral group [23]. The absorption band which around 465–480 cm^{-1} is due to

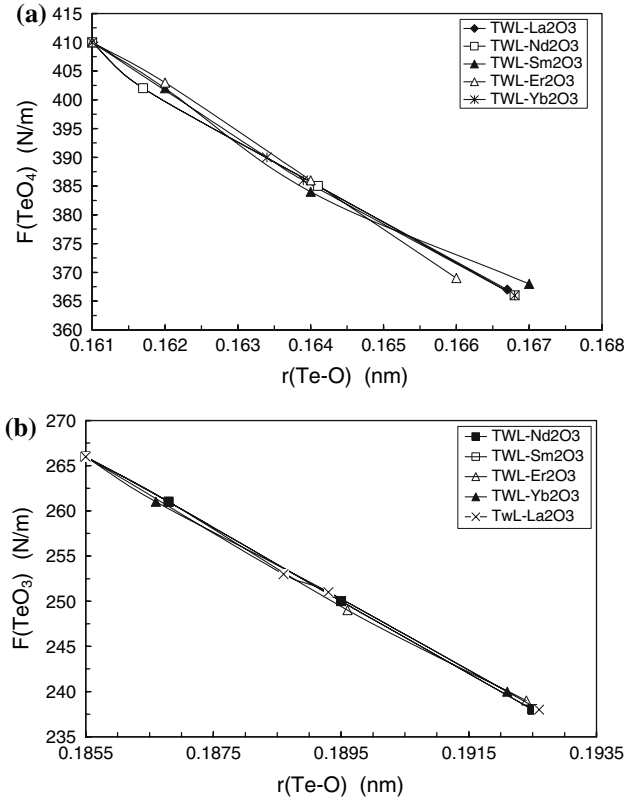

Fig. 3 Variation of stretching force constant of **a** TeO_4 and **b** TeO_3 groups with the bond length of the studied glasses

TeO_4 group and 339–348 cm^{-1} due to v_4 of TeO_4 group. The weak band at 150–120 cm^{-1} of the present glasses may relate to the Li_2O vibrations [26]. It should be noted that there is broad shoulder on this band, which is centred at 135 cm^{-1}. The very strong peak with a maximum, which at between 48–57 cm^{-1}, is identified with the Boson Peak,

Table 5 Raman absorption band position of some of TeO_2–WO_3–Li_2O glasses doped with rare earth oxides

Sample no.	Boson peak	Li–O	TeO_3	v_4 of TeO_4	TeO_4	v_1 of TeO_4	TeO_4	v_1 of WO_4
TWL	54	132	220	360	480	700		930
TWLNd1	48	153		342	470	705		930
TWLNd3	48	135		345	480	700	740	930
TWLEr1	48	150		342	480	702		930
TWLEr3	57	135		345	480	695	745	930
TWLSm1	48	135		348	480	711		930
TWLSm3	57	120	234	339	470	700	740	930
TWLYb1	48	126		342	460	705		930
TWLYb3	54	144		345	475	700	745	930
TWLLa1	51	135	220	342	460	708		930
TWLLa3	54	138		348	465	700	735	930

a feature characteristic of the vitreous state. Although various attempts have been made to explain the origin of the Boson Peak, it is generally accepted that it can be related to long-range spatial correlations in the structure [27]. The disorder resulting from the creation of the glass network yields a change in selection rules of the equivalent order state, thus allowing the activity of acoustic modes in the Raman spectrum [28]. The peak intensity and the band position of the Boson peak are shown in Fig. 5. It is shown that they are in reverse behaviour. This leads to that the Boson peak is affected by the rare earth oxide additions. It is also seen that the TeO_4 band position (695–711 cm^{-1}) shifts to higher wavenumber (lower frequency) by introduce the rare earth oxides to the present glass. This attributed to that the rare earth oxides will enter the glass network as intermediate. The peak around 360 cm^{-1} can

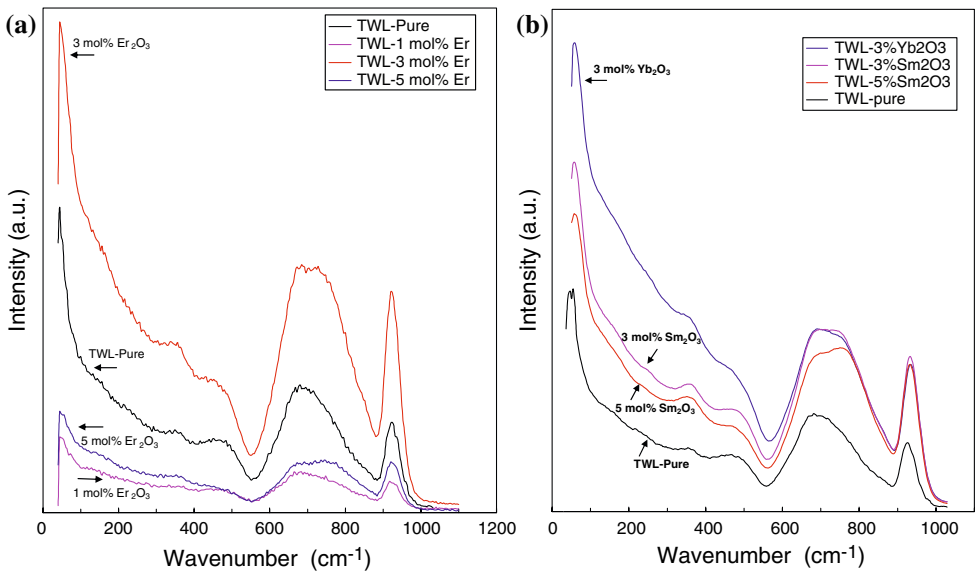

Fig. 4 **a** Raman spectra of Er_2O_3 doped TeO_2–WO_3–Li_2O glass. **b** Raman spectra of Te_2O–WO_3–Li_2O glasses doped with (Sm_2O_3,Yb_2O_3)

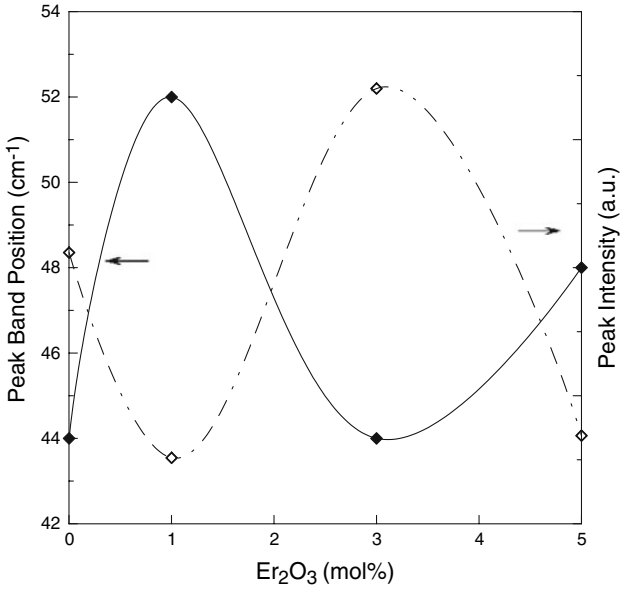

Fig. 5 Variation of Boson peak band position and intensity with composition of the Er-doped glass

be assigned to both TeO_3 tp and/or Er–O bond [25]. The formation of Te–O–W bonds is expected, because both Te and W ions have comparable electronegativity values (2.1 and 2, respectively) and can, therefore, substitute for each other in bonding with O atoms. Peak at 930 cm^{-1} is assigned to the WO_4 tetrahedra and/or WO_6 octahedra.

Conclusions

In the present work, tellurite glasses has been prepared according to this formula $(70 - x)TeO_2$–$20WO_3$–$10Li_2O$–xLn_2O_3 where $x = 0$, 1, 3 and 5 mol.% and Ln are La, Pr, Nd, Sm, Er and Yb, respectively. The increase in density and molar volume of the present quaternary telluride glasses when the rare earth oxides added is due to the higher molecular weight of the added rare earth oxides than that of TeO_2. The density correlated with the calculated cross-link density of the glasses. The Poisson's ratio was also calculated. The calculated number of bonds per unit volume of the glasses was increase and the glass become more rigid. The bond length between the ions of the main structural groups of the glass was calculated and the wavenumber band position of the absorption bands is also calculated. The structure of these glasses is built up from TeO_4 tbp, TeO_3 tp, WO_4 tetrahedral and/or WO_6 octahedra groups. The low frequency Raman absorption band obtained for all the studied samples, which at around 50 cm^{-1}, are identified with Boson peak, a feature characteristic of the vitreous state. This means that the rare earth ions were incorporated in the network of the present glasses and acts as a network intermediate. Also it can be suggested that the present glasses are good host for these rare earth ions and good for optical properties and optical applications.

Acknowledgements The authors thank M. Poulain for the lab facilities.

References

1. Elliott SR (1990) Physics of amorphous materials, 2nd edn. Longman Scientific, Essex, England
2. Nasu H, Matsushita O, Kamiya K, Kobayashi H, Kubodera K (1990) J Non-Cryst Solids 124:275
3. Hirao K, Kishimoto S, Tanaka K, Tanabe S, Soga N (1992) J Non-Cryst Solids 139:151
4. Kim SH, Yoko T, Sakka S (1993) J Am Ceram Soc 79:865
5. Lambson E, Saunders G, Bridge B, El-Mallawany R (1984) J Non-Cryst Solids 69:117
6. El-Mallawany R (2002) Tellurite glass handbook: physical properties and data. CRC Press, FL (International Materials Institute for New Functionality in Glass (IMI-NFG), Lehigh University, USA (2005)). www.lehigh.edu/imi/resources.htm
7. El-Mallawany R (1992) J Appl Phys 72:1774
8. El-Mallawany R, Patra A, Friend Ch, Kapoor R, Prasad PN (2004) Opt Mater 26:267
9. Sooraj Hussain N, Hungerford G, El-Mallawany R, Gomes MJM, Lopes MA, Ali N, Santos JD, Buddha S (2008) J Nanosci Nanotechnol 8:1
10. Moawad HM, Jain H, El-Mallawany R (2009) J Phys Chem Solids 70:224
11. El-Mallawany R, Dirar Abdalla M, Abbas Ahmed I (2008) Mater Chem Phys 109:291
12. El-Mallawany R (1989) Infrared Phys 29:781
13. Ozdanova J, Ticha H, Tichy L (2007) J Non-Cryst Solids 353:2799
14. El-Mallawany R (1998) Mater Chem Phys 53:93
15. Mackishima A, Mackenzie JD (1975) J Non-Cryst Solids 17:147
16. Higazy A, Bridge B (1985) J Non-Cryst Solids 72:81
17. El-Mallawany R (2000) Mater Chem Phys 63:109
18. Rajendran V, Plainville N, Modak DK, Chaudhuri BK (2000) Phys Status Solidi A 180:467
19. Mochida N, Takahashi K, Nakata K, Shibusawa S (1978) Yogyo-Kyokai-Shi 86(1):24
20. Sekiya T, Mochida N, Siejima A (1995) J Non-Cryst Solids 191:115
21. Charto P, Gengembre L, Armand P (2002) J Solid State Chem 168:175
22. Shaltout I, Tang Y, Braunstein R, Abu-Elazm AM (1995) J Phys Chem Solids 56:141
23. Hager IZ, El-Mallawany R, Poulain M (1999) J Mater Sci 34:5163. doi:10.1023/A:1004799510599
24. El-Hofy M, Hager IZ (2000) Phys Status Solidi A 182:697
25. Kamatsu T, Tawaragama H, Mohri H, Matusita K (1991) J Non-Cryst Solids 135:105
26. Sekiya T, Mochida N, Ohtsuka A, Tonokawa M (1992) J Non-Cryst Solids 144:128
27. Malinvsky VK, Sokolov AP (1986) Solid State Commun 57:757
28. Duverger C, Romain F, Bouazaoui M, Turrell S (1997) J Mol Struct 410:285